Clin. Cardiol. 23, 115–122 (2000)

Comparison of Left Ventricular Diastolic Filling with Myocyte Bulk Modulus Using Doppler Echocardiography and Acoustic Microscopy in Pressure-Overload Left Ventricular Hypertrophy and Cardiac Amyloidosis

HISASHI MASUGATA, M.D., KATSUFUMI MIZUSHIGE, M.D., SHOICHI SENDA, M.D.,* AKI KINOSHITA, M.D., HARUHIKO SAKAMOTO, M.D.,† SEIJI SAKAMOTO, M.D., HIROHIDE MATSUO, M.D.

Second Department of Internal Medicine, *Department of Primary Care Medicine, and †Second Department of Pathology, Kagawa Medical University, Kagawa, Japan

Summary

Background: The myocardial bulk modulus has been described as the constitutive properties of the left ventricular (LV) wall and is measured as ρV^2 (ρ = density, V = sound speed) using acoustic microscopy.

Hypothesis: The study was undertaken to assess the relationship between the myocyte bulk modulus and transmitral inflow patterns in patients with pressure-overload LV hypertrophy (LVH) and cardiac amyloidosis (AMD).

Methods: In 8 patients with LVH, 8 with AMD, and 10 controls without heart disease, the transmitral inflow pattern was recorded by Doppler echocardiography before death, and myocardial tissue specimens were obtained at autopsy. The tissue density and sound speed in the myocytes were measured by microgravimetry and acoustic microscopy, respectively. The diameters of the myocytes were measured on histopathologic specimens stained by the elastica Van Gieson method.

Results: In the subendocardium, the myocyte bulk modulus was larger in LVH (2.98×10^9 N/m^2, $p < 0.001$) and smaller in AMD (2.61×10^9 N/m^2, $p < 0.001$) than in the controls (2.87×10^9 N/m^2). The myocyte diameter in LVH (26 ± 1 μm) was larger than that in the control (21 ± 1 μm, $p < 0.001$) and AMD (20 ± 1 μm, $p < 0.001$). The bulk modulus in the subendocardial myocyte significantly correlated with the deceleration time (DT) of the early transmitral inflow ($r = 0.689$, $p = 0.028$ in control, $r = 0.774$, $p = 0.024$ in LVH, and $r = 0.786$, $p = 0.021$ in AMD).

Conclusion: The changes in the myocyte elasticity as represented by the bulk modulus were limited to the subendocardial layers and may be related to relaxation abnormalities in LVH and a reduction in LV compliance in AMD.

Key words: transmitral inflow, left ventricular hypertrophy, cardiac amyloidosis, acoustic microscopy, myocardial bulk modulus, left ventricular compliance

Introduction

Left ventricular (LV) diastolic filling dynamics have been evaluated based on pressure–volume relationships.[1–3] We have postulated in addition that the myocyte bulk modulus of elasticity as a constitutive property is an important factor regulating the pressure–volume relationship and diastolic filling dynamics. Recently, the scanning acoustic microscope with high-frequency ultrasound has been applied to measuring the bulk modulus of biological materials, including the myocardium,[4,5] kidney,[6] and arterial wall.[7] This instrument permits the visualization of tissues on a microscopic scale as well as the measurement of the sound propagation speed in the region of interest on the microscopic image. With this information, the myocyte bulk modulus can be calculated easily.

In patients with LV hypertrophy[8] and with cardiac amyloidosis,[9] abnormalities of LV diastolic filling can be demon-

Address for reprints:

Katsufumi Mizushige, M.D.
Second Department of Internal Medicine
Kagawa Medical University
1750-1, Miki, Kita
Kagawa 761-0793, Japan

Received: March 16, 1999
Accepted with revision: June 22, 1999

strated by analyzing the transmitral inflow pattern recorded by Doppler echocardiography.[10, 11] We, therefore, selected autopsy patients with pressure-overload left ventricular hypertrophy (POLVH) and cardiac amyloidosis in whom Doppler echocardiographic studies were performed before death. Our intent was (1) to measure the myocyte bulk modulus of elasticity using acoustic microscopy, and (2) to evaluate its relationship with LV diastolic filling as assessed by the transmitral inflow patterns.

Methods

Subjects

The study population included 26 patients consisting of 10 patients (mean age 61 years, range 54–69 years) without cardiovascular diseases who made up the control group, 8 patients (mean age 65 years, range 58–70 years) with POLVH, and 8 patients (mean age 65 years, range 54–71 years) with cardiac amyloidosis. The patients with POLVH had a history of hypertension (15 ± 5 years) and showed LV hypertrophy with a mean wall thickness of > 13 mm for the interventricular septum and posterior wall; in addition, these patients had a normal ejection fraction on M-mode echocardiograms. Eight of 10 control patients and 6 of 8 patients with POLVH were receiving chemotherapy with one or more of the following medications: mitomycin C, 5-fluorouracil, adriamycin, and cisplatin. The drugs and their dosages were not different between the control and POLVH groups. All patients with hypertension were free from antihypertension drugs during admission. The cardiac amyloidosis was diagnosed by cardiac biopsy in five patients and by rectal biopsy in three patients. The postmortem diagnosis of cardiac amyloidosis was confirmed by histopathologic examination in all patients (Table I).

Specimen Preparation

Specimens of the LV wall at the level of the mitral valve chorda were obtained for measurement of the bulk modulus and histopathology at autopsy. The specimens were fixed in a solution of 10% neutral buffered formalin, embedded in paraffin, and sectioned at a thickness of 4 μm. The deparaffinized and unstained sections were imaged, and the tissue sound speed was measured with an acoustic microscope. After the acoustic microscopic examination, the specimens underwent a light microscopic examination.

Acoustic Microscope

An acoustic microscope (HSAM-500S; Hitachi, Co., Ltd., Tokyo, Japan) with a 450-MHz transducer containing piezoelectric film and an acoustic sapphire lens was used. The lateral and axial resolutions were approximately 2.2 and 0.8 μm, respectively.[12] The unstained specimen was placed on a horizontal stage and scanned by the transducer. Deionized water provided acoustic coupling of the acoustic lens to the specimen. The reflected signals were received by the same transducer and entered for display on a computer monitor (Fig. 1).

Horizontal plane image: The transducer could be scanned horizontally in X-Y directions to produce C-mode two-dimensional images. The focus setting of the lens was determined by ascertaining the point of maximal output of the reflected wave form on the oscilloscope, and X-Y scanning was always conducted horizontally across a focal plane. We set the focus on the surface of the specimen. The structure of the myocardium was clearly visible on the acoustic microscope images at × 30–× 500 magnification (Fig. 2, upper section of the acoustic microscopic image).

X-Z image: The transducer could also be shifted vertically. The depth setting of the lens was gradually altered as it traversed back and forth along the same X-axis to produce an X-Z-mode image. There was an interference fringe at every $\lambda_M/2$ spacing (λ_M = acoustic wave length in the medium) at the point where there was connecting fluid, but no sample. The images were produced by the interference of the superimposed wave reflected from different interfaces (i.e., the surface of the stage and the surface of the lens). Since the interference fringe shifts depended on the propagation delay in the sample at any point on the X-axis line where the sample existed, the acoustic propagation speed was measured from this fringe shift (Fig. 2, lower section of the acoustic microscopic image). The interference image was input into the on-line computer image analyzer, and the magnitude of all fringe shifts on the X-axis line set was automatically measured from the endocardial or epicardial border of the myocardium to each 3 mm inner point. The average value of all fringe shifts was used for calculation of the sound speed by the following formula:[12–14]

$$Vs = Vw(1-\Delta z/ds)$$

where Vs is the sound speed of the specimen, Vw is the sound speed of the coupling water, Δz is the magnitude of the fringe shift, and ds is the thickness of the specimen (4 μm) (Fig. 2). The sound speed was measured on five X-axis lines in each specimen, and the mean value was used for the analysis.

Bulk modulus: The myocyte bulk modulus (N/m^2) of elasticity was defined by:

$$\rho V2$$

where ρ is the density (g/cm^3) and V is the sound speed (m/s).

The density of the myocardium in the same area in which the acoustic microscopic examination was carried out was measured by microgravimetry. Seven pieces of sample were obtained by a 1.0 mm punch and placed in a bromobenzene-kerosene density gradient column[15] that was calibrated daily with potassium sulfate standards. The position of the sample indicating the density was determined 2 min after insertion. The density of each sample was determined by linear regression analysis. The highest and lowest values were excluded, and the mean density was calculated based on the values in the remaining five samples.

TABLE I Clinical characteristics and Doppler echocardiographic data for all patients

	Age	Cause of death	Time delay (days)	HR (beats/min)	S/D BP (mmHg)	M-mode echo data					Doppler data				
						IVS (mm)	PW (mm)	Mass (g)	LVD (mm)	EF (%)	E (cm/s)	A (cm/s)	E/A	DT (ms)	IVRT (ms)
Control															
1	54	Pancreatic ca.	31	78	128/76	10	9	285	47	66	55	55	1.00	140	60
2	60	Hepatoma	25	72	110/70	12	10	299	45	62	52	75	0.69	200	90
3	55	Hepatoma	14	76	140/80	12	11	285	43	60	55	52	1.06	160	80
4	58	Pancreatic ca.	37	68	138/68	8	7	259	49	70	72	72	1.00	200	80
5	64	Stomach ca.	12	84	116/60	11	10	272	44	65	35	60	0.58	210	90
6	58	Leukemia	8	88	116/66	10	8	313	50	72	58	87	0.67	200	70
7	66	Uterine ca.	23	70	120/84	10	9	222	42	73	70	88	0.80	150	80
8	66	Lung ca.	46	66	130/86	11	10	343	49	66	82	90	0.91	180	80
9	60	Hepatoma	40	90	132/82	12	10	313	46	68	40	50	0.80	220	90
10	69	Lung ca.	7	77	118/74	8	7	285	51	61	48	60	0.80	180	80
Mean	61.0		24	77	125/75	10.4	9.1	288	47	66	57	69	0.83	184	80
±SD	±5.0		±14	±8	±10/9	±1.5	±1.4	±33	±3	±4	±15	±16	±0.16	±27	±9
POLVH															
1	69	Lung ca.	28	70	146/88	15	13	343	42	66	40	80	0.50	360	120
2	65	Hepatoma	14	68	140/70	14	12	375	46	70	52	70	0.74	300	100
3	58	Leukemia	9	88	160/80	13	13	359	45	74	38	60	0.63	280	100
4	62	Liver cirrhosis	12	92	158/86	16	13	343	41	60	66	58	1.14	230	75
5	66	Hepatoma	11	84	120/62	15	12	425	48	61	44	80	0.55	260	110
6	62	Pancreatic ca.	48	80	142/60	16	13	425	46	59	38	78	0.49	230	120
7	64	Lung ca.	22	72	112/80	14	12	375	46	68	48	68	0.71	250	90
8	70	Cerebral hemorrage	18	78	136/72	17	13	343	40	63	60	72	0.83	210	80
Mean	64.5		20	79	141/75	15.0[a]	12.7[a]	373[a]	44	65	48	71	0.70	265[a]	99[b]
±SD	±3.9		±13	±9	±21/10	±1.3	±0.5	±34	±3	±5	±10	±9	±0.22	±48	±17
AMD															
1	54	Heart failure	12	90	100/60	16	14	359	41	50	74	10	7.40	110	35
2	58	Heart failure	36	88	118/72	15	13	359	43	55	75	30	2.50	160	50
3	60	Heart failure	17	92	102/78	14	13	359	44	52	75	33	2.30	140	50
4	63	Heart failure	33	76	112/80	17	15	375	40	49	77	18	4.28	150	30
5	59	Heart failure	15	82	108/76	16	14	425	45	51	88	28	3.14	120	40
6	65	Heart failure	5	74	116/70	14	12	375	46	57	75	38	1.97	150	55
7	71	Heart failure	20	84	112/74	15	13	299	39	48	70	28	2.50	1.70	45
8	68	Heart failure	14	98	106/76	13	12	359	46	53	90	42	2.14	145	50
Mean	62.3		19	86	109/73	15.0[a]	13.2[a]	364[a]	43	52[a]	78[b]	28[a]	3.28[a]	143[c]	44[a]
±SD	±5.6		±11	±8	±6/6	±1.3	±1.0	±34	±3	±3	±7	±10	±1.82	±20	±9

[a] $p < 0.001$.

[b] $p < 0.01$.

[c] $p < 0.05$ vs. control.

Abbreviations: Control = patient without cardiovascular disease, POLVH = patient with pressure-overload left ventricular hypertrophy, AMD = patient with amyloidosis, Time delay = interval between Doppler examination and autopsy, HR = heart rate, S/D BP = systolic/diastolic blood pressure, IVS = interventricular septum, PW = posterior wall, LVD = left ventricular dimension, EF = ejection fraction, DT = deceleration time of E wave, IVRT = isovolumetric relaxation time, ca. = cancer, SD = standard deviation.

The myocyte bulk modulus was compared with the LV diastolic function estimated by Doppler echocardiographic variables recorded before death.

Histopatholgy

The sections used for acoustic microscopy were subsequently stained by the elastica Van Gieson method for light microscopy. Cross sections of the myocytes at × 400 magnification were input into a Macintosh computer (Power Mac, Apple, Inc., Cupertino, Calif., USA) and were digitized using a NIH Image software. The measurement system was calibrated by digitizing the images of a standardized micrometer. The myocyte diameter was measured as the short axis width of the myocyte across the nucleus of 20 discrete myocytes at each subendocardial or subepicardial region of the left ventricle. The mean myocyte diameter was used for the analysis.

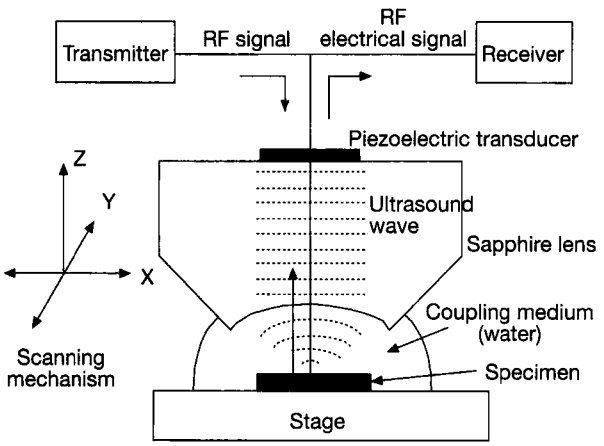

FIG. 1 Block diagram of acoustic microscope. RF = radiofrequency.

Doppler Echocardiographic Measurements

The time between the Doppler echocardiographic study and autopsy was retrospectively within 48 days, and no significant difference among the three groups was observed. The LV end-systolic and end-diastolic dimensions and the ventricular septal and LV posterior wall thickness were measured on M-mode echocardiogram. The LV ejection fraction, the mean LV wall thickness [(septal thickness + posterior wall thickness)/2] and LV mass [1.04 × (septal thickness + LV dimension + posterior wall thickness)^3 − 13.6] were calculated.

On the transmitral inflow pattern recorded by pulsed Doppler flowometry, the peak flow velocities during early diastole (E) and atrial contraction (A), and early to late peak velocity ratio (E/A) were measured. The deceleration time of the E wave was measured as the time from peak velocity to extrapolation of the decline to baseline. In addition, the isovolumetric relaxation time was measured as the time interval from the onset of the second heart sound to the onset of mitral inflow (Fig. 3).

Statistical Analysis

All data are reported as mean ± standard deviation. All statistical tests were performed with the use of statistical software (STATVIEW-J4, Abacus Concepts, Berkeley, Calif., USA). Differences between the subendocardial and subepicardial regions in all groups were examined using the Student's *t*-test for paired data. Differences among groups were assessed using ANOVA. Scheffe's test was used after the ANOVA to determine which pairs had significant differences. Correlations between the elastic bulk modulus and Doppler measurements were assessed by a linear regression analysis. A p value of < 0.05 was taken to indicate a significant difference.

Results

Doppler Echocardiographic Data

The mean values for LV wall thickness in patients with POLVH and cardiac amyloidosis were significantly greater than for the control group ($p < 0.001$, $p < 0.001$, respectively). No significant difference in mean LV wall thickness was observed between POLVH and amyloidosis. Ejection fraction in patients with POLVH was not different from that in the control group, but ejection fraction in patients with amyloidosis was significantly lower than that in the control group ($p < 0.001$) (Table I).

No significant difference in E/A between POLVH and control was observed. The deceleration time of the E wave and the isovolumetric relaxation time in POLVH were prolonged compared with those in the control group ($p < 0.001$, $p < 0.01$, respectively). In patients with amyloidosis, E/A was significantly larger ($p < 0.001$), and the deceleration time of the E wave and the isovolumetric relaxation time were shorter than those in the control group ($p < 0.05$, $p < 0.001$, respectively) (Table I, Fig. 3).

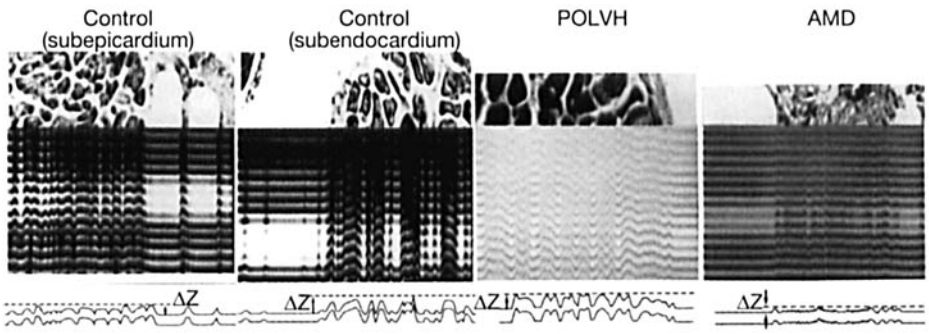

FIG. 2 Horizontal plane image and X-Z inference mode image with its schematic illustration in control, POLVH, and AMD. The transducer was scanned vertically and transversely along the X-axis, bottom edge of the horizontal plane image, and X-Z mode images were produced indicated as middle panels. Δz = magnitude of the fringe shift, Control (subepicardium) = subepicardium in control patient, Control (subendocardium) = subendocardium in control patient, POLVH = subendocardium in patient with pressure-overload left ventricular hypertrophy, AMD = subendocardium in patient with amyloidosis.

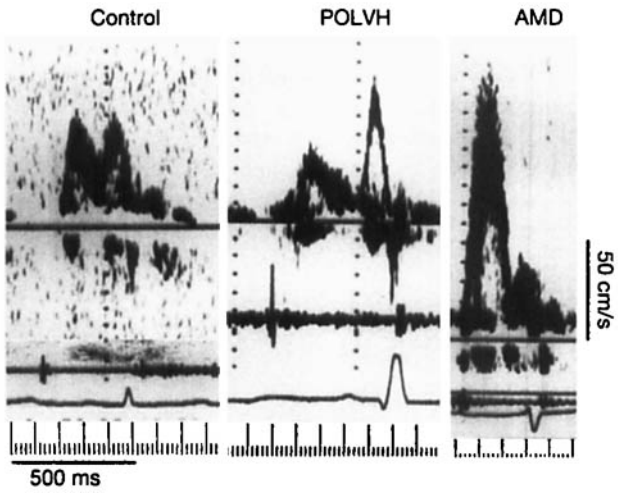

FIG. 3 Transmitral inflow velocity pattern recorded by Doppler echocardiography in control, POLVH, and AMD. Abnormal relaxation pattern in POLVH and restrictive pattern in AMD, respectively, were represented. Control = patient without cardiovascular disease, POLVH = patient with pressure-overload left ventricular hypertrophy, AMD = patient with amyloidosis.

Acoustic Properties of Myocardial Tissue

A fringe shift on the X-Z image was observed at the site of the myocyte, but not at the interstitium, as confirmed on the X-Y (horizontal plane) acoustic microscopic image. In the subendocardial region, the sound speed was higher ($p<0.001$) and the density of the myocardial tissue was greater ($p<0.001$) in patients with POLVH, and the sound speed and density in patients with amyloidosis were lower ($p<0.001$) than in the control. The myocyte bulk modulus in patients with POLVH was larger ($p<0.001$), and that in amyloidosis was lower ($p<0.001$) than in the control (Table II). In the subepicardial region, no significant difference in bulk modulus was observed among the control, POLVH, and amyloidosis groups. The bulk modulus in the subepicardium was significantly lower than that in the subendocardium in the control and POLVH groups (both $p<0.001$) and larger in the amyloidosis group ($p<0.001$).

Relationship between Cardiac Function and Bulk Modulus

In the subendocardial region, the deceleration time of the E wave correlated significantly with the bulk modulus in the control group ($r=0.689$, $p=0.028$), in POLVH ($r=0.774$, $p=0.024$), and in amyloidosis ($r=0.786$, $p=0.021$) (Fig. 4). In the subepicardial region, however, no indices of Doppler echocardiography correlated with the bulk modulus.

Histopathology

In patients with POLVH, mild interstitial fibrosis and hypertrophic myocytes were observed on the image stained by the elastica Van Gieson method. In the subendocardial region, the mean myocardial cell diameter in patients with POLVH (26 ± 1 μm) was larger than that in the control group (21 ± 1 μm) ($p<0.001$), and that in patients with amyloidosis (20 ± 1 μm) was not different from that in the control group. In the subepicardial region, no significant difference in the mean myocyte diameter was observed among the three groups (20 ± 2 μm in control, 22 ± 2 μm in POLVH, and 19 ± 1 μm in amyloidosis). In patients with amyloidosis, interstitial amyloid de-

TABLE II Sound speed, density, and elastic bulk modulus of myocardial tissue in control and in patients with pressure-overload left ventricular hypertrophy, and patients with cardiac amylodidosis

	Subendocardial region		
	Control (n = 10)	POLVH (n = 8)	AMD (n = 8)
Sound speed (m/s)	1626 ± 8	1653 ± 11 [a]	1560 ± 10 [a, b]
Density (g/cm^3)	1.084 ± 0.003	1.090 ± 0.002 [a]	1.071 ± 0.003 [a, b]
Elastic bulk modulus ($\times 10^9$ N/m^2)	2.87 ± 0.04	2.98 ± 0.04 [a]	2.61 ± 0.04 [a, b]
	Subepicardial region		
	Control (n = 10)	POLVH (n = 8)	AMD (n = 8)
Sound speed (m/s)	1603 ± 11 [c]	1607 ± 10 [c]	1597 ± 9 [c]
Density (g/cm^3)	1.080 ± 0.002 [c]	1.081 ± 0.001 [c]	1.079 ± 0.002 [d]
Elastic bulk modulus ($\times 10^9$ N/m^2)	2.78 ± 0.04 [c]	2.79 ± 0.04 [c]	2.75 ± 0.04 [c]

[a] $p<0.001$ vs. control.
[b] $p<0.001$ vs. POLVH.
[c] $p<0.001$ and [d] $p<0.1$ vs. the corresponding value in subendocardial region.
Abbreviations as in Table I.

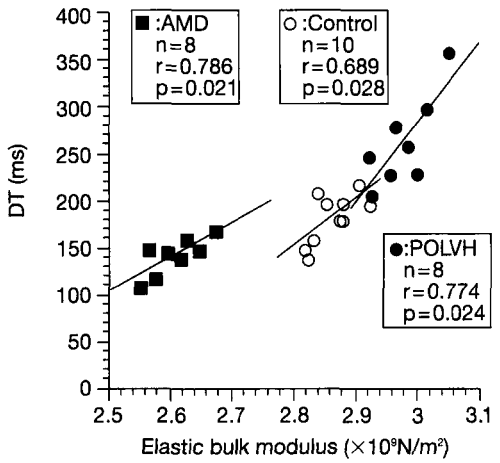

FIG. 4 Correlation between deceleration time of early inflow velocity curve and elastic bulk modulus of subendocardial myocyte in control, POLVH and AMD. Significant correlation was observed in each group. DT = deceleration time of early inflow velocity curve. Other abbreviations as in Figure 3.

posits and degenerated myocardial cells were observed, and these changes were predominant in the subendocardial region (Fig. 5).

Discussion

Calculation and Determinants of Myocyte Bulk Modulus

The sound speed through a tissue, which is the major determinant of the elastic bulk modulus, is affected by biochemical constituents such as protein, water, and fat.[16] In particular, an increase in protein content has been reported to accelerate the sound speed in various tissues.[17] In the present study, we were able to determine the myocyte sound speed by measuring the amplitude of a fringe shift on the X-Z image, with the observations being made for myocytes. We therefore considered that the sound speed measured by the acoustic microscope reflected the protein concentration in the myocyte.

In patients with hypertension, previous studies[18,19] as well as the present histopathologic study have demonstrated concurrent increases in myocyte diameter and protein content; these results indicate an augmentation of protein synthesis in response to pressure loading. Our results show the interesting fact that the accelerated sound speed in POLVH is accompanied by myocyte hypertrophy, resulting in an increase in the bulk modulus of elasticity.

In amyloidosis, myocyte degeneration is caused by a great infiltration of amyloid fibers.[20,21] Although the myocyte diameter did not decrease in the present study, the decrease in the sound speed in the subendocardial myocyte probably indicates a reduction in the intracellular protein synthesis of the myocyte resulting from myocyte degeneration. Moreover, the reduction in the myocyte bulk modulus in patients with amyloidosis suggests that the ventricular wall becomes less elastic and more fragile due to cellular degeneration.

Difference in Tissue Elasticity between Subendocardium and Subepicardium

Hypertension places increased tension on the inner surface of the left ventricle, and pressure load may directly affect the structure of the subendocardium. In hypertension, mechanical stimulation may subsequently be greater in the subendocardium than in the subepicardium, and a resultant myocyte hypertrophy that can be detected as an increased bulk modulus is predominant in the subendocardium. In contrast, mechanical loading may augment the damage to myocytes in the subendocardium in the amyloid heart. The transmural differences in the myocyte bulk modulus in the present study are in agree-

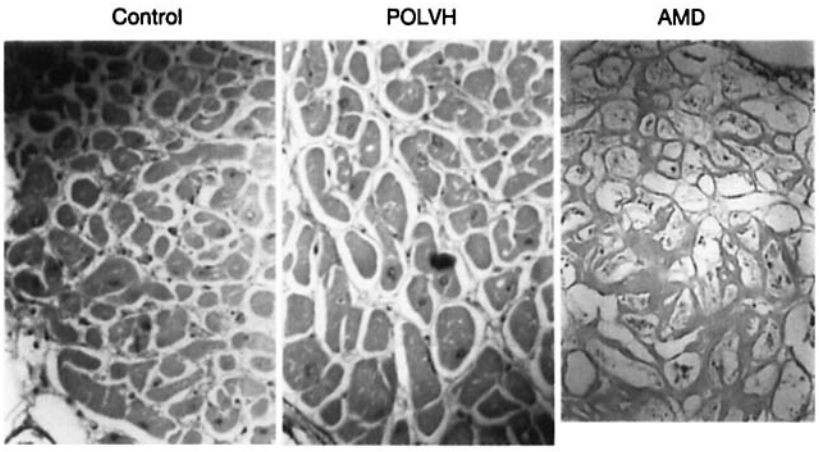

FIG. 5 Histopathology of subendocardium stained by elastica Van Gieson method. Mild interstitial fibrosis and hypertrophic myocyte in patients with POLVH, and interstitial amyloid deposit and degenerated myocardial cells in AMD, respectively, were observed. Abbreviations as in Figure 3.

ment with the results of a previous histopathologic study,[22] that demonstrated that amyloid deposition and myocyte degeneration are mainly observed in the subendocardial region.

Conclusively, it is considered that an alteration in myocyte constitutive properties reflects the loading conditions for the LV wall and suggests that the subendocardial side may have a large effect on LV diastolic function.

Bulk Modulus and Diastolic Filling in Pressure-Overload Left Ventricular Hypertrophy and Amyloidosis

In POLVH, a low E velocity, a prolongation of the deceleration time, and an abnormal relaxation have been observed.[23] Because the ventricular relaxation is a complex of energy-dependent processes, and because the myofibrils return to their original length, two possible mechanisms have been proposed for an abnormal relaxation in POLVH. The first involves the likelihood of myocardial ischemia induced by an increased demand and insufficient supply, a mismatch of the hypertrophied myocardium with the microvasculature. In the present study, however, although hypertrophied myocytes and an increase in bulk modulus were observed, damage to the microvasculature or myocyte changes induced by ischemia were not observed histopathologically.

The second possible mechanism involves an alteration in the constitutive properties of cardiac muscle cells. The type of proteins produced by pressure overloading are more suited for tension development than for shortening, and Zile *et al.*[24] have demonstrated that a viscous damping can be changed in pressure-hypertrophied cardiocytes using an agarose gel-stretch method. In the present study, changes in protein concentration were identified based on increases in the sound speed and the bulk modulus of the myocytes, which might be concordant with an increase in protein suited to tension development and a resulting impairment of relaxation.

In cardiac amyloidosis, Arbustini *et al.*[21] have demonstrated that a decrease in cell diameter and a degenerative feature with myofilament loss can be recognized by electron micrograph. The structural changes produced by amyloid deposition likely result in a decrease in protein concentration in the myocyte, which was observed as a reduction in the bulk modulus in the present study.

The myofilament damage and interstitial deposition of amyloid fibrils decreases the effective operative chamber compliance of the left ventricle, which can result in progressive diastolic dysfunction. In the late stage of diastolic dysfunction, as effective operative compliance decreases, the E velocity on the transmitral inflow velocity curve gradually increases and the deceleration time shortens. A pseudonormal pattern appears, and the advances of disease produce a restriction in the filling pattern.[10, 25] In the present study, a positive correlation was observed between the deceleration time of the E wave and the bulk modulus. This shows that the myocyte becomes less elastic due to the accumulation of amyloid substances and that the degeneration of the myocyte may play a role in reducing LV compliance.[26]

Limitations

Since most of the control and patients with POLVH died of malignancy, the effects of chemotherapy and malnutrition could not be completely discounted. However, no significant difference in the treatment for malignancy was observed between the control and POLVH groups. In addition, systolic dysfunction and cardiac atrophy were not shown in either group. Therefore, the influence of chemotherapy or malnutrition was small in our results.

The tissue used in this study was formalin fixed, and it is known that such a preparation increases the sound speed by 0.5%.[27] Therefore, formalin fixation may increase the tissue elastic bulk modulus. In addition, Tamura *et al.*[28] have reported that the bulk modulus of skeletal muscle fibers obtained in solution is $2.4–2.6 \times 10^9$ N/m^2. The higher values of myocardial tissue elasticity in the present study may be attributed to the dehydration process that occurs during specimen preparation.

However, there have never been any methods directly measuring the tissue elasticity at the myocyte level of the heart. Even if formalin fixation and dehydration affects the results of the bulk modulus measurements, we believe that tissue elasticity could be evaluated at least as a relative value and that its relationship with LV diastolic function could be analyzed.

Conclusions

We have demonstrated that the myocyte bulk modulus of the subendocardium is higher in patients with pressure-overload left ventricular hypertrophy and lower in patients with cardiac amyloidosis than in control patients; in the subepicardial region, however, the values are similar. The myocyte bulk modulus of elasticity in the subendocardial region correlates with the deceleration time of the transmitral E velocity; this correlation may have different meanings in LV hypertrophy or cardiac amyloidosis. In LV hypertrophy, this correlation is regulated by the process of impaired relaxation, and in amyloidosis the correlation is related to a reduction in LV compliance. This is the first report analyzing the relationship between LV diastolic function and the myocyte bulk modulus of elasticity.

References

1. Courtois M, Vered Z, Barzilai B, Ricciotti NA, Pérez JE, Ludbrook PA: The transmitral pressure-flow velocity relation: Effect of abrupt preload reduction. *Circulation* 1988;78:1459–1468
2. Thomas JD, Weyman AE: Echocardiographic Doppler evaluation of left ventricular diastolic function: Physics and physiology. *Circulation* 1991;84:977–990
3. Nishimura RA, Tajik J: Evaluation of diastolic filling of left ventricle in health and disease: Doppler echocardiography is the clinician's Rosetta stone. *J Am Coll Cardiol* 1997;30:8–18
4. O'Brien WD Jr, Sagar KB, Warltier DC, Rhyne TL: Acoustic propagation properties of normal, stunned, and infarcted myocardium. Morphological and biochemical determinants. *Circulation* 1995; 91:154–160
5. Saijo Y, Tanaka M, Okawai H, Sasaki H, Nitta S, Dunn F: Ultrasonic tissue characterization of infarcted myocardium by scanning acoustic microscopy. *Ultrasound Med Biol* 1997;23:77–85

6. Sasaki H, Tanaka M, Saijo Y, Okawai H, Nitta S, Suzuki K: Ultrasonic tissue characterization of renal cell carcinoma tissue. *Nephron* 1996;74:125–130
7. Kameyama K, Asano G: Evaluation of elastic structural change in coronary atherosclerosis using scanning acoustic microscopy. *Atherosclerosis* 1992;94:191–200
8. Maron BJ, Spirito P, Green KJ, Wesley YE, Bonow RO, Arce J: Noninvasive assessment of left ventricular diastolic function by pulsed Doppler echocardiography in patients with hypertrophic cardiomyopathy. *J Am Coll Cardiol* 1987;10:733–742
9. Klein AL, Hatle LK, Burstow DJ, Seward JB, Kyle RA, Bailey KR, Luscher TF, Gertz MA, Tajik AJ: Doppler characterization of left ventricular diastolic function in cardiac amyloidosis. *J Am Coll Cardiol* 1989;13:1017–1026
10. Rakowski H, Appleton C, Chan KL: Canadian consensus recommendations for the measurement and reporting of diastolic dysfunction by echocardiography: From the investigators of Consensus on Diastolic Dysfunction by Echocardiography (review). *J Am Soc Echocardiogr* 1996;9:736–760
11. Garcia MJ, Thomas JD, Klein AL: New Doppler echocardiographic applications for the study of diastolic function. *J Am Coll Cardiol* 1998;32:865–875
12. Ishikawa I, Kanda H, Katakura K: An acoustic microscope for subsurface detect characterization. *IEEE Trans Sonics Ultrasonics* 1985;SU-32:325–331
13. Chubachi N, Kushibiki J, Sannomiya T, Akashi N, Tanaka M, Okawai H, Dunn F: Scanning acoustic microscope for quantitative characterization of biological tissue. *Acoust Imag* 1987;16: 277–285
14. Kinoshita A, Senda S, Mizushige K, Masugata H, Sakamoto S, Kiyomoto H, Matsuo H: Evaluation of acoustic properties of the live human smooth muscle cell using scanning acoustic microscopy. *Ultrasound Med Biol* 1998;24:1397–1405
15. Marmarou A, Poll W, Shulman K, Bhagavan H: A simple gravimetric technique for measurement of cerebral edema. *J Neurosurg* 1978;49:530–537
16. Pohlhammer JD, O'Brien WD Jr: The relationship between ultrasonic attenuation and speed in tissues and the constituents: Water, collagen, protein, and fat. In *Medical Physics of CT and Ultrasound: Tissue Imaging and Characterization*, (Eds. Fullerton GD, Zazebski JA), p.409–435. New York: American Institute of Physics, 1980
17. Dunn F: Ultrasonic properties of biological media. In *Ultrasound Interactions in Biology and Medicine* (Eds. Melner R, Rosenfield E, Cobet U), p.1–6. New York: Plenum Publishing Corp., 1983
18. Wong K, Boheler KR, Petrou M, Yacoub MH: Pharmacological modulation of pressure-overload cardiac hypertrophy. Changes in ventricular function, extracellular matrix, and gene expression. *Circulation* 1997;96:2239–2246
19. Weber KT, Janicki JS, Pick R, Abrahams C, Shroff SG, Bashey RI, Chen RM: Collagen in the hypertrophied, pressure-overloaded myocardium. *Circulation* 1987;75(suppl I):I-40–I-47
20. Roberts WC, Waller BF: Cardiac amyloidosis causing cardiac dysfunction: Analysis of 54 necropsy patients. *Am J Cardiol* 1983;52: 137–146
21. Arbustini E, Merlini G, Gavazzi A, Grasso M, Diegoli M, Fasani R, Bellotti V, Marinone G, Morbini P, Dal Bello B, Campana C, Ferrans VJ: Cardiac immunocyte-derived (AL) amyloidosis: An endomyocardial biopsy study in 11 patients. *Am Heart J* 1995;130: 528–536
22. Pellikka PA, Holmes DR Jr, Edwards WD, Nishimura RA, Tajik AJ, Kyle RA: Endomyocardial biopsy in 30 patients with primary amyloidosis and suspected cardiac involvement. *Arch Intern Med* 1988;148:662–666
23. Villari B, Vassalli G, Schneider J, Chiariello M, Hess OM: Age dependency of left ventricular diastolic function in pressure overload hypertrophy. *J Am Coll Cardiol* 1997;29:181–186
24. Zile MR, Richardson K, Cowles MK, Buckley JM, Koide M, Cowles BA, Gharpuray V, Cooper G IV: Constitutive properties of adult mammalian cardiac muscle cells. *Circulation* 1998;98: 567–579
25. Nishimura RA. Miller FA Jr, Callahan MJ, Benassi RC, Seward JB, Tajik AJ: Doppler echocardiography: Theory, instrumentation, technique, and application. *Mayo Clin Proc* 1985;60:321–343
26. Klein AL, Hatle LK, Taliercio CP, Oh JK, Kyle RA, Gertz MA, Bailey KR, Seward JB, Tajik AJ: Prognostic significance of Doppler measures of diastolic function in cardiac amyloidosis. A Doppler echocardiography study. *Circulation* 1991;83:808–816
27. Bamber JC, Hill CR, King JA, Dunn F: Ultrasonic propagation through fixed and unfixed tissues. *Ultrasound Med Biol* 1979;5: 159–165
28. Tamura Y, Suzuki N, Mihashi K: Adiabatic compressibility of myosin subfragment-1 and heavy meromyosin with or without nucleotide. *Biophys J* 1993;65:1899–1905